Phreatomagmatic eruption during the buildup of a Triassic carbonate platform (Oman Exotics): eruptive style, associated deformations, and implications on CO2 release by volcanism

Christophe Basile, François Chauvet

Phreatomagmatic eruption during the buildup of a Triassic carbonate platform (Oman Exotics): eruptive style, associated deformations, and implications on CO_2 release by volcanism

Christophe Basile (corresponding author), François Chauvet
Laboratoire de Géodynamique des Chaînes Alpines, CNRS UMR 5025
Observatoire des Sciences de l'Univers de Grenoble, Université Joseph Fourier
Maison des Géosciences, 1381 rue de la Piscine
38400 St Martin d'Hères, France
tel. 334 765 140 69; fax 334 765 140 58
email cbasile@ujf-grenoble.fr; francois.chauvet@ujf-grenoble.fr

Abstract
Oman exotics represent remnants of a Triassic carbonate platform (Misfah Formation). Within these carbonates, and coeval with the sedimentation, several basaltic magmatic events occurred mainly as intrusions, also as lava flows and projections. We describe one of these events, that produced a phreatomagmatic eruption along a volcanic fissure. The initial ascent of magma probably occurred along on a normal fault related to gravity-driven sliding of the carbonates towards the platform edge. Magma first emplaced in a saucer-shaped sill few tens of meters below the surface. This intrusion provided a decollement layer, that may have speed up the gravity-driven sliding, opening fractures that brought sea-water in contact with the magma, hence triggering the phreatomagmatic eruption. Eruption was followed by the collapse of the limestones in a megabreccia infilling the eruptive line and prohibiting further contact between sea water and magma. The main magma volume emplaced at depth in two superposed magma chambers that replaced the host sediments and uplifted the overlying eruptive line. These magma chambers fossilized the substratum of the carbonate platform, that consists in uplifted sediments from the distal Hawasina basin. Replacing limestones by magma chambers may have release huge volumes of Carbon dioxide, estimated to be two to three hundred times higher than CO_2 release by volcanic gases. CO_2 release by decarbonating sediments may be an important mechanism to explain climatic changes associated to some large igneous provinces such as Siberia, Central Atlantic Magmatic Province, or Karoo, where very large magmatic volumes where intruded in sedimentary basins.

Keywords
Phreatomagmatic eruptions; sills; magma chambers; megabreccia; carbonate platforms; Carbon dioxide;

INTRODUCTION

Carbonate platforms commonly developped above or on the side of marine volcanos, either in intraplate setting (e.g. Hess, 1946; Hamilton, 1956; Matthews et al., 1974; Schlager, 1981; Buigues et al., 1992; Premoli Silva, Haggerty, Rack et al., 1993; Sager, Winterer, Firth et al., 1993) or in subduction-related volcanic arcs (e.g. Fulthorpe and Schlanger, 1989; Larue et al., 1991; Watkins, 1993; Soja, 1996). However, in most studied cases, the carbonate platform builded on an inactive volcano. There is only sparse observations of interactions between volcanism and carbonate platform sedimentation, mainly restricted to interstratification of sediments and lava flows or volcanic projections (e.g. Buigues et al., 1992; Soja, 1996; Beltramo, 2003) or exceptionally to shallow-marine eruption through a carbonate platform (MIT guyot: Shipboard Scientific Party, 1993; Martin et al., 2004). It seems obvious that volcanism coeval with carbonate platform build-up may strongly, but locally, influence the sedimentation. On the other hand, one can expect that sediment-magma interaction may have some implications on gas-releases during volcanic eruptions, which are suspected to trigger climatic changes (e.g. Wignall, 2001). As carbonates represent the main reservoir in the Carbon atmospheric cycle, their interaction with magmas may imply significant modifications of atmospheric release of CO_2 by volcanism.

In this paper we describe how a volcanic eruption interacted with the formation of a Triassic carbonate platform in Oman, emphasizing on small- and large-scale deformations of lithified and unlithified sediments, magmatic intrusions, deposition of volcano-sedimentary formations, consequences on local subsidence and subsequent carbonate sedimentation, and a rough estimate of CO_2 release from the sediments.

GEOLOGICAL SETTING

As part of the southern margin of the Neo-Tethys ocean, the Oman continental margin formed during Permian-Triassic times (Béchennec, 1988; Robertson and Searle, 1990; Sengör et al., 1993). Palinspatic reconstructions suggest the development of contrasted sedimentary environments since Middle Permian times, with a continental platform (Saiq Formation: Glennie et al., 1974), a continental slope (Sumeini Formation: Glennie et al., 1974), and basinal environments (Hawasina Formations: Glennie et al., 1974; Béchennec, 1988). All these sedimentary units were thrusted on the arabian platform during the upper Cretaceous obduction of the Sumail ophiolites (Béchennec et al., 1988) (Fig. 1). It is noteworthy that the paleopositions of the sedimentary units on the continental margin were mainly derived from their positions in the tectonic pile, assuming an outward thrust sequence (Glennie et al., 1973,

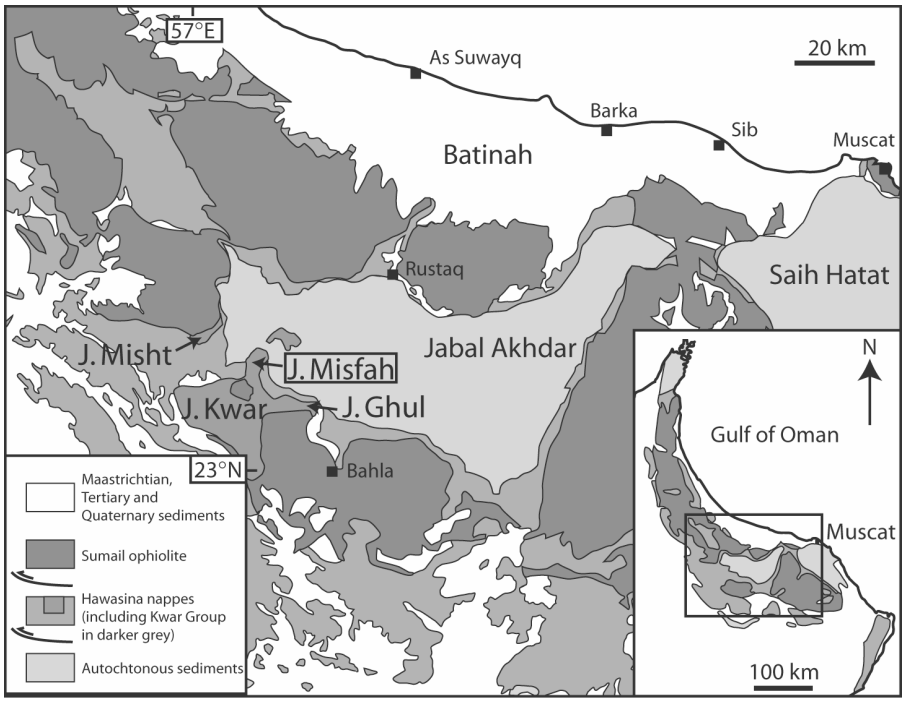

Figure 1: Location of the studied area (Jabal Misfah, boxed) in a simplified geological map of central and eastern Oman Mountains (modified after Béchennec et al., 1990). Inset: simplified geological map of northern Oman, modified after Glennie et al., 1974.

1974; Béchennec, 1988; Robertson and Searle, 1990). There is an ongoing debate on the nature of the basement below the Hawasina basin, supposed to be either oceanic (Glennie et al., 1973, 1974; Stampfli et al., 1991; Pillevuit et al., 1997), continental (Béchennec, 1988; Béchennec et al., 1990, 1991) or intermediate (Graham, 1980; Searle and Graham, 1982). As a consequence, the Permian (e.g. Pillevuit et al., 1997) or Triassic (e.g. Béchennec, 1988) age for the onset of the oceanic accretion is also a matter of debate.

During Triassic times, a carbonate platform developped within the Hawasina basin. Remnants of this platform were named Oman Exotics by Glennie et al. (1974), and referred to the Kwar Group by Béchennec (1988). In the Hawasina nappes, the Kwar Group crops out mainly south of the western termination of Jabal Akhdar anticline in several mountains dominated by high carbonate cliffs: Jabal Misht, Jabal Misfah, Jabal Kwar, Jabal Ghul (Fig. 1). This Group has been divided by Béchennec (1988) into four Formations, later-on subdivided into six Formations by Pillevuit (1993). Stratigraphy has been defined on the northern and eastern slopes of Jabal Misfah, and comprises from bottom to top (Fig. 2):

(i) A volcanic unit, made of massive pillow lavas basalts, hyaloclastites and tuffites, and dated Ladinian-Carnian from foraminifera found in few intercalated limestones (Pillevuit, 1993). This unit thrusts the Late Permian to Liasic bathyal sediments of Al Jil (limestones and cherts) and Matbat (limestones, sandstones and siltstones) Formations (Beurrier et al., 1986).

(ii) The Misfah Formation, made of thinly bedded marly limestones at the base (Subayb Formation, Pillevuit, 1993), overlain by thick and massive platform limestones. These two members were dated respectively Ladinian-Carnian, and Ladinian-Carnian to Rhaetian by Pillevuit (1993). Krystyn (in Baud et al., 2001) proposed a revised age of Middle-Late Norian for the lower member, and topmost Norian-Rhaetien for the upper member. Few intercalations of conglomeratic tuffites occur in the lower part of Misfah Formation, also intruded by basaltic dikes and sills.

(iii) The Jurassic to Cretaceous Fatah (Pillevuit, 1993), Nadan and Safil pelagic Formations.

OBSERVATIONS

Stratigraphy

The studied volcano-sedimentary section belongs to the lowest part of Misfah Formation, north-east of Jabal Misfah, near the village of Subayb. It may belong to the Subayb Formation as defined by Pillevuit (1993), but we do not support this stratigraphic terminology as both published reference sections appeared to be limited upward by tectonic contacts. The volcanic and sedimentary log described here (Fig. 2) synthesizes observations from the northeastern part of Jabal Misfah, once removed the numerous and more recent magmatic intrusives and fault offsets. However, it is important to note that while carbonates have and important lateral extension, effusive as intrusive magmatic formations occur only locally.

Above submarine basaltic lava flows (pillow lavas and hyaloclastites), the sedimentary section begins by few beds of volcanic gravels in a carbonate matrix. Then a first carbonate unit develops with from bottom to top ten meters of decimeter-thick beds of yellow marly limestones, forty meters of wavy-bedding marly limestones, two meters of marls, and fifteen meters of thirty centimeters-thick grey limestones strata. These carbonates are locally truncated by a twelve meters-thick volcano-sedimentary unit including from bottom to top tuffites, volcanic breccia, sub-marine lava flows and peperites. Above begins a second carbonate unit, approximately one hundred and fifty meters-thick, made of thirty centimeters-thick beds of black limestones with few white stromatolithic layers. Two thin volcano-sedimentary layers are intercalated within this carbonate unit. They consist mainly in tuffites, with volcanic and sedimentary clasts, separated by few limestone beds exhibiting numerous sliding structure. According to Pillevuit (1993), this second carbonate unit has deposited at shallow depths, mainly in the tidal zone. In the following description of the volcanic event, the various parts of this second carbonate unit are referred to as (from bottom to top) lower limestones, lower tuffs, intermediate

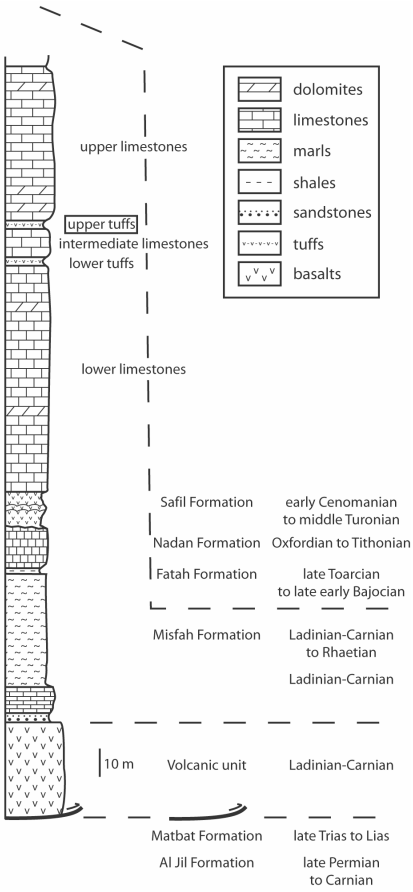

Figure 2: Stratigraphy of th Kwar Group. Lithologic log i detailed only in the lowest part o Misfah Formation (see text fo details). Ages according to L vu et al. (1997) and E rier a (1986). The d m mat ver is related pper s (b d).

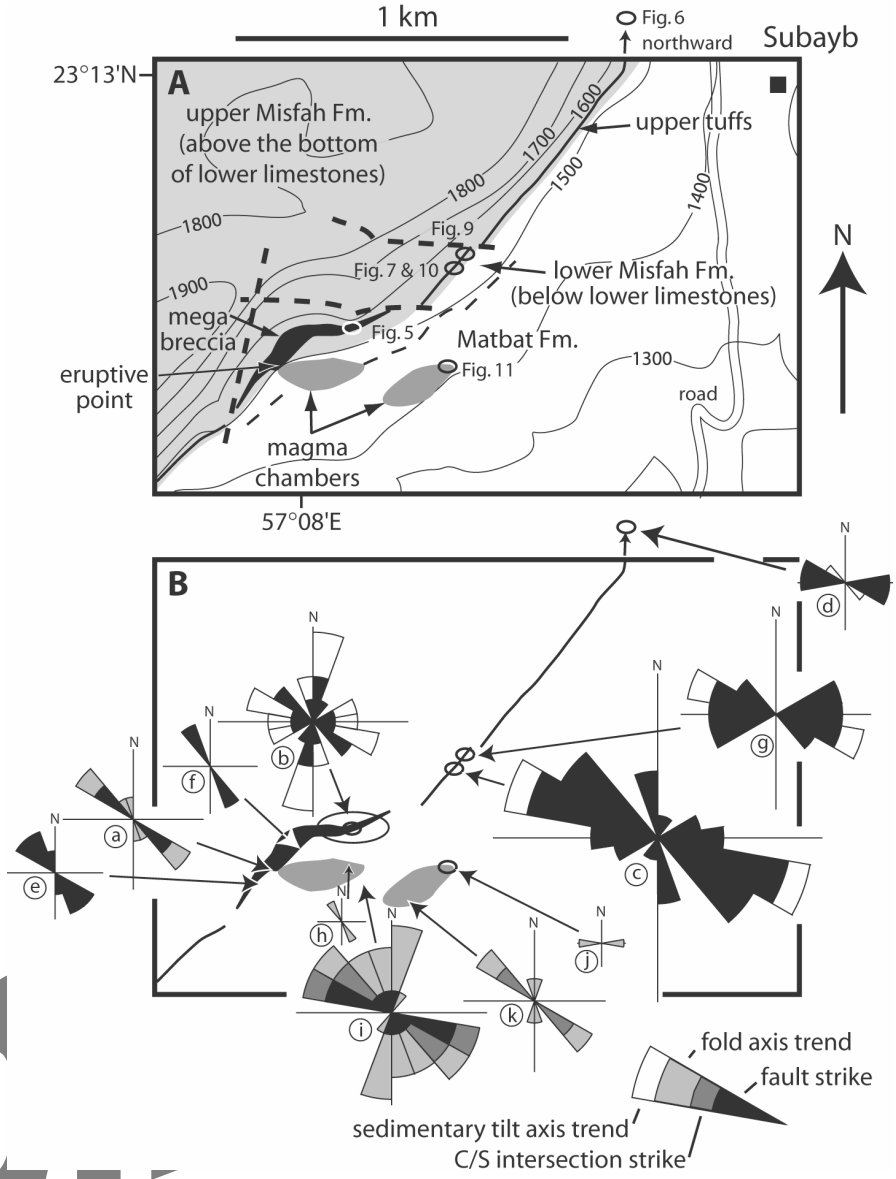

Figure 3: (A) Schematic geological map of the studied area. Topography (meters) from Beurrier et al., 1986. Thick stippled lines are recent faults, thin stippled line represents the unobserved limit between Misfah and Matbat formations. Figures 5 to 7 and 9 to 11 are located by ellipses. (B) Same as Figure 3A, with location of the upper tuffs, megabreccia and magma chambers and rose diagrams of structural observations. Rose diagrams (a) to (k), see comments in the text. Same scale for all rose diagrams, maximum seven values on rose c. All structural measurements are related to the same magmatic event, with the exception of N-S structures at sites (i) and (k) which are related to a more recent eastward normal shear.

limestones, upper tuffs, and upper limestones (Fig. 2).

Magmatic event

Eruption

The volcanic eruption we describe in this paper was associated with the deposition of the upper tuffs. At the eruptive point, the lower limestones were totally removed (Figs. 3A and 4). On each side of the eruptive point, the lower limestones and the lower tuffs were eroded in a 300 meters-wide zone. Erosion was more effective on the northeastern side. Southwest of the eruptive point, the lowest part of the lower limestones were cut by a normal fault striking N130° (Fig. 3B-a, Fig. 4). The removed limestones formed a megabreccia over the erosional surface, with meter- to decameter-scale blocks of limestones tilted in an intraformational breccia made by angular blocks of the eroded limestones mixed in a grey limestone matrix (Fig. 5). It is noteworthy that some basaltic gravels were encountered within the limestone breccia, but that there is no volcanic nor volcano-detritic layer between the megabreccia and the erosional surface. The megabreccia is lateraly continuous with the intermediate limestones, where in situ brecciation also occurred. In all breccias, the sliding blocks are made at least partly by dolomite beds, probably more lithified at the time of the eruption. Sliding planes and syn-sedimentary tilt axis in the megabreccia and intermediate limestones are predominantly striking either N110° or N-S (Fig. 3B-b to d, Fig. 6). They are sliding towards the eruptive point,

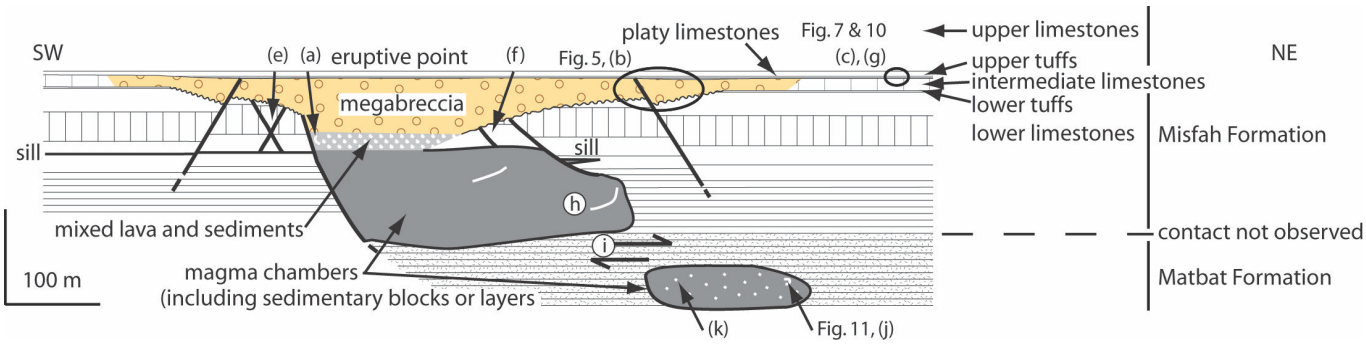

Figure 4: Section across the eruptive point, reconstructed at the time of deposition of the upper limestones. Figures 5, 7, 10 and 11, and rose diagrams (a) to (k) (Figure 3) are located by ellipses or arrows. White dots and lines in the magma chambers represent sedimentary blocks and layers, respectively.

with the exception of a structure observed as far as 1.8 km northeast of the eruptive center (Fig. 3B-d, Fig. 6). The megabreccia, its tilted blocks and associated sliding structures are sealed by the upper tuffs.

In the vicinity of the eruptive point, the upper tuffs thicken to 15 meters. Here few meters of platy limestones seal the breccia (Fig. 4). They are covered by intercalation of thin tuffite beds with massive breccia made of limestones and few basaltic blocks in a calcareous matrix. In the overlying upper carbonates, there is no lateral variations of facies nor thicknesses. In the platy limestones we observed several syn-sedimentary listric faults that indicate NNE-SSW extension and sliding towards the eruptive point (Fig. 3B-c, Fig. 7). The megabreccia vanishes away from the eruptive point and the upper tuffs thin to few meters. There, in the first decimeters of the upper tuffs, numerous shells from an underlying lumachelle are mixed with limestones clasts in a calcareous matrix. Although the volcanic elements are a minor component in the tuffs, glassy or palagonitized shards were homogeneously found in the tuff matrix, together with armored elongated lapilli and some isolated or armored spinel crystals. Lapilli cores are either calcareous, or derived from volcanic fragments or vesicular glass. The edges of lapilli cores are very irregular, corroded and underlined by oxidation. Lapilli rims also include palagonized shards in a cryptocristalline matrix showing concentric structures (Fig. 8). The thinly layered tuffs exhibit basaltic and limestone clasts, as big as one meter in diameter. The asymetric impact sags show that the blocks were ejected from the eruptive point and fall on previously deposited tuffs (Fig. 9). The same displacement of ejecta from the eruptive point towards N10° is indicated by oblique bedding in small dunes (Fig. 10).

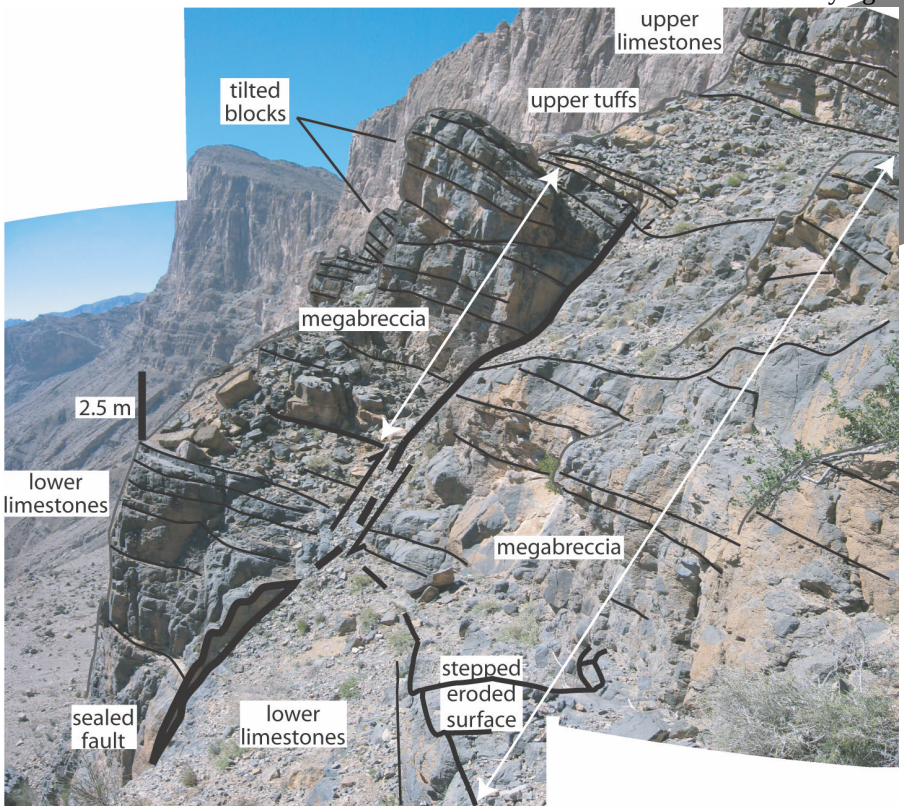

Figure 5: View towards southwest of the megabreccia. Indicative scale (beware the perspective). Note the tilted blocks within the megabreccia, its stepped and erosive basal surface, and the normal fault sealed by the upper tuffs. The upper part of Misfah Formation forms the cliffs in the background. Structural observations made in this area are shown Figure 3B in rose diagram (b). Location Figures 3 and 4.

Faulting

During the magmatic event, some normal faults affected the underlying limestones (Fig. 4). These faults were all sealed by the upper tuffs. Some conjugated normal faults striking N155° occurred on both sides of the eruptive point (Fig. 3B-e and f), but northward the significant throws are located on north-dipping normal faults, while southward the southernmost fault dips south. On each side of the eruptive point, the closest normal faults does not shift the erosive base of the megabreccia, while farther faults shift it (Figs. 4 and 5). These normal faults define a small horst centered on the eruptive

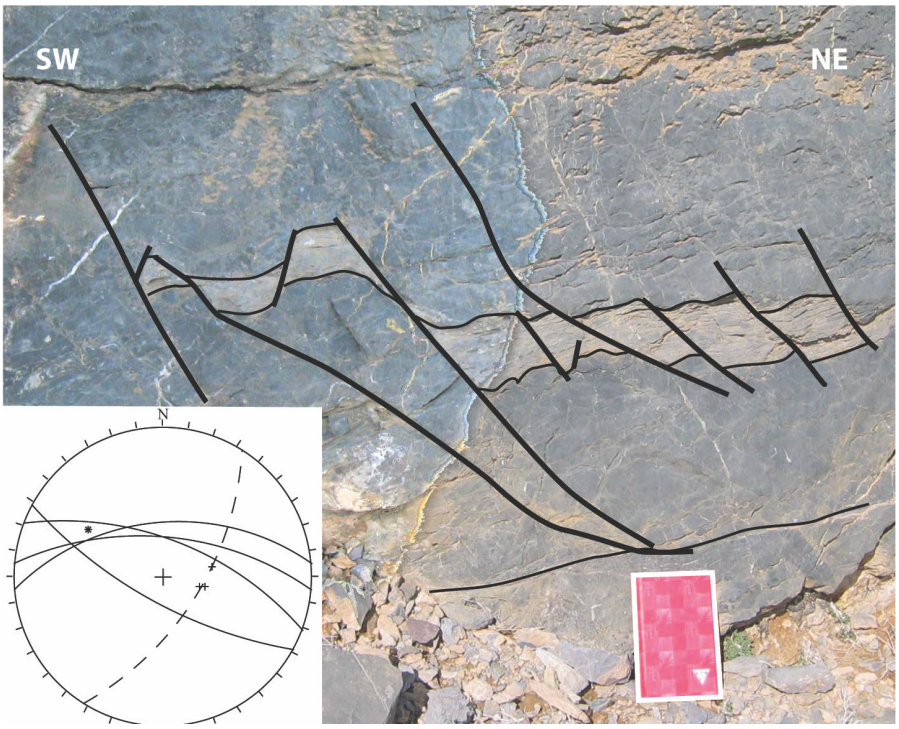

Figure 6: Syn-diagenetic normal faults in the intermediate limestones, indicating sliding towards N30°. Wulff net (lower hemisphere): small crosses are poles for bedding, gread circles are normal faults, stippled great circle and star are the best great circle for bedding and its pole (i.e. the axis of rotation), respectively. Notebook for scale (17.5 cm-high, 11.5 cm-wide). Structural measurements are also shown Figure 3B in rose diagram (d). Approximate location Figure 3.

point. It is noteworthy that the strike of the normal faults sligthly changes from N160° southwestward to N110° northeastward, while the NNE-SSW stretching direction indicated by the rotation of the upper tuff layers does not significantly change (Fig. 3B-a to g).

Magma chambers

Within the eruptive point, folded beds of limestones are mixed together with a basaltic breccia containing numerous calcareous clasts and blocks. Folds are roughly cylindrical, with sub-horizontal axial surfaces and axis trending N130° to N150° (Fig. 3B-a). Right below the eruptive point, screes do not allow to observe the deep structures, which can only be seen northward below the lower limestones. There a magma chamber replaces the underlying wavy-bedding limestones (Figs. 3A and 4). In the magma chamber, blocks or beds of the enclosing or overlying limestones are mixed with basalts. Some limestone beds are longer than 40 m, and folded with N150°-trending axis (Fig. 3B-h). Overlying limestones clearly fell down inside the magma chamber. It explains the rise of the magma chamber hanging wall in the lower limestones towards the eruptive point. Locally, a pinching out sill accommodates the incipient rotation of a limestone block at the side of the magma chamber (Fig. 4). N130°-trending dikes in the enclosing limestones similarly show how they were replaced by the magma chamber. During a more recent magmatic event, a basaltic dike striking N20° and N-S calcite veins were emplaced through the magma chamber. The basalts are quite homogeneous in the magma chamber, with the exception of an increasing alteration toward the surface, probably in relation with higher water content at the time of the magmatic event. No trace of a magma chamber has been found south of the eruptive point, but a basaltic sill underlines the base of the lower limestones (Fig. 4). While horizontal, this sill is offset by a normal fault sealed by the upper tuffs.

Below the magma chamber, few tens of meters of pelagic silicified limestones and sandstones attributed to the Matbat Formation were deformed by two successive ductile deformations: normal shearing towards N50° characterized the older one; N-S trending folds represent a younger eastward normal shear (Fig. 3B-i). It is important to note that there is no significant shear zone between the Matbat limestones and the overlying magma chamber, but a ductile mix of magma and sediments. Below these deformed sediments, similar limestones beds and blocks

Figure 7: Syn-sedimentary deformation in the platy limestones, indicating sliding towards N190° to N220°. Same legend as for Figure 6 for the stereo net; the thick great circle represents the sedimentary dike. Same notebook as for Figure 6. Structural observations made in and around this outcrop are shown Figure 3B in rose diagram (c). Location Figures 3 and 4.

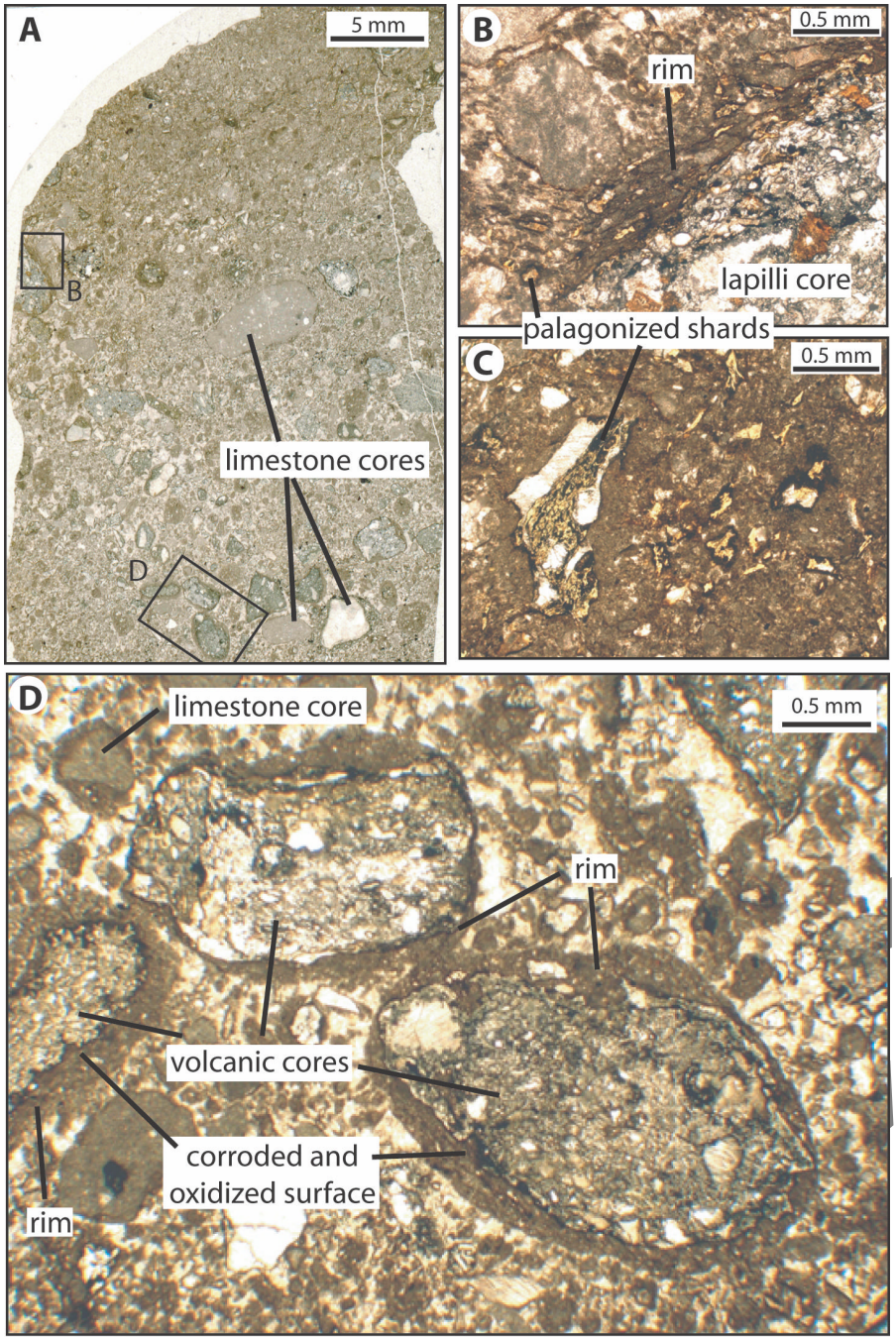

Figure 8: Texture of the upper tuffs. A: scanned thin section. B: lapilli rim with yellowish glassy shards in a cryptocristalline matrix. C: glassy shards palagonized and oxided in the tuffs matrix. D: armoured lapillis with altered volcanic cores. Note the corroded edges of the volcanic fragments. Figures 8B and 8D are located in Figure 8A; Figure 8C is a detail from an other thin section.

from the Matbat Formation are included inside a second magma chamber, where radiolarites were also found as xenoliths. As in the upper magma chamber, sedimentary beds are often folded, with fold axis trending N90° to N140° (Fig. 3B-j, Fig. 11). Shear zones indicate top-to-N50° displacements (Fig. 3B-k). The sedimentary blocks or layers are clearly metamorphosed in this lower magma chamber, while they are not at macroscopic scale in the upper one.

INTERPRETATION

Structure

The eruptive point and the upper and lower magma chambers appear lined up in a WNW-ESE direction parallel to the main normal faults (Fig. 3B). This feature can not be fitted by a crater, i.e. a circular structure centered on the eruptive point. As this linear disposition is parallel or sub-parallel with the normal fault bounding the eruptive point, with the other major normal faults, and with the shear zones at depth, it suggests that both magmatic and tectonic processes were associated in a NE-SW extensional tectonic regime. The magma probably rose to the subsurface not in a pipe but along a WNW-ESE-trending fissure. What appears as an eruptive point on the Jabal Misfah may be in fact a section in an eruptive line.

We also observed slight changes in the strike of the main normal faults, from N160° in the southwestern part of the outcrop, to N110° eastwards or northeastwards (Fig. 3B). Moreover, N110°-striking normal faults are in some places associated with N-S-striking normal faults or sliding structures (Fig. 3B-b and c). These N110° and N-S structures may have been formed as conjugated faults in a transtensional regime, indicating a N60° lengthening direction, perpendicular to N160° normal faults. Both changes in orientation and transtension can be explained by an homogeneous displacement on an arcuate structure (Fig. 12): in the central part, displacement is perpendicular to the structure, and results in N110°-striking normal faults in an extensional regime; on the sides, displacement becomes oblique, and can be partitioned in divergence perpendicular to the structure, and strike-slip parallel to the structure. The resulting faults are either controled by the transtensional tectonic regime (conjugated N110°- and N-S-striking faults), or by the local topography imposed by the main structure (N160°-striking normal faults, parallel to the main structure). This interpretation suggests that the eruptive line may be curved, several kilometers-long, and formed in a northeastward displacement.

Moreover, several observations indicate an asymmetry in the deformation: the lower limestones are more thinned and the normal faults more numerous north of the eruptive line than southward, the main normal faults are dipping northeast as the fault

Figure 9: Ballistically-emplaced limestone block. The grey limestone blocks were projected in the tuffs. The white limestones blocks are screes from the above cliff. Same notebook as for Figure 6. Structural observations made around this outcrop are shown Figure 3B in rose diagram (g). Location Figure 3.

bounding the eruptive line, the deep shear zones also indicate displacements toward NE. This suggests that the carbonate platform was stable southwest of the eruptive line, while the northeastern part slided northeastward on the intrusive magma and a deep shear zone, possibly towards the edge of the carbonate platform.

Evolution

It's also possible to reconstruct in detail how the magmatic event proceeded (Fig. 13):

- At the beginning, the magma rose to the bottom of the lower limestones, probably along an incipient normal fault (Fig. 13-A). The magma intruded as sub-horizontal sills in the main discontinuities of the sedimentary section, especially at the bottom of the lower limestones. Unfolding of the structure indicates that the first magmatic intrusion was saucer-shaped (Chevallier and Woodford, 1999), and probably fed from the proto-magma chamber, as in the central feeding model proposed by Thomson and Hutton (2004). While there is no direct evidence for it, it is assumed that the two magma chambers initiated in the same time. At this stage, there is no evidence of explosion associated with sill intrusion, suggesting the absence of aquifer at magma depth.

- The increasing size of the magmatic intrusion may have allow the overlying carbonates to slide on the proto-magma chamber (Fig. 13-B). This destabilization may have open tension cracks, that brought sea-water in contact with the magma. The resulting phreatomagmatic explosion removed the overlying sediments on the normal fault hanging wall (Fig. 13-C). Several observations point to a sub-aerial eruption: well-bedded and locally dune-bedded sediments, impact sags (Fisher, 1977), base surge suggested by in situ erosion and resedimentation of shells at the bottom of the tuffs.

- At surface, this explosion may have produce a trench, and the surface and sub-surface sediments may have slide towards this trench, inducing instantaneously in-situ brecciation by breaking and sliding of the more lithified beds, mixed in a lime mud matrix (Fig. 13-D). This megabreccia lies on an erosional surface, that represents the lower limit of the unstable sediments, and that cross-cut the intermediate limestones, the lower tuffs, the upper part of the lower limestones, and the normal faults which are closest to the eruptive line. The fact that the conjugated normal faults south of the eruptive line do not cut the saucer-shaped sill suggests that they formed when the magma was still fluid in the sill, and consequently that the eruption was sub-contemporaneous with the intrusion.

- Back-stripping the present day section indicates that these sealed normal faults do not accommodate the subsidence of the northeast block, but

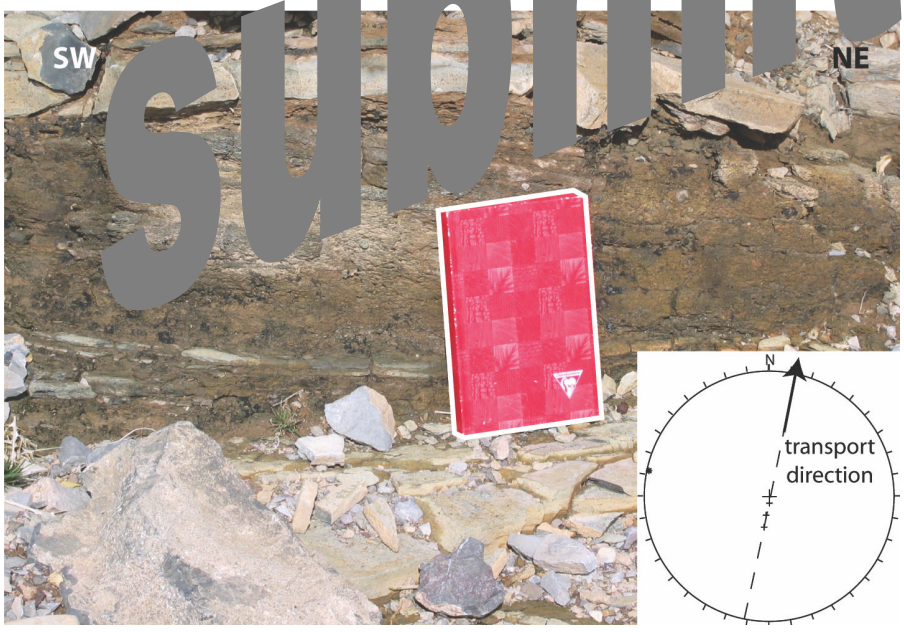

Figure 10: Dune structure in the upper tuffs. Same notebook and same legend for the stereo net as for Figure 6. Location Figures 3 and 4.

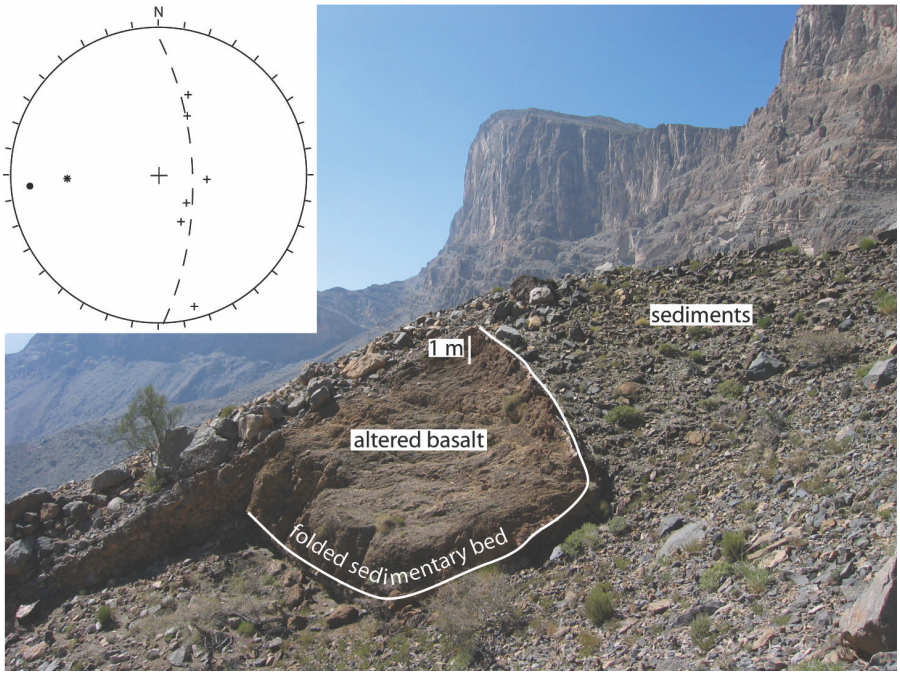

Figure 11: Folded sedimentary bed within the lower magma chamber (view towards WSW). Same legend for the stereo net as for Figure 6; the black dot and the star represent the measured and computed fold axis, respectively. The fold axis is also shown Figure 3B in rose diagram (j). Location Figures 3 and 4.

the uplift of a narrow horst centered on the eruptive line, contemporaneous with the eruption, but prior to the redeposition of the megabreccia. Normal faults farther of the eruptive line shift the bottom of the megabreccia, but are sealed at its top (Fig. 13-E). They define a wider horst formed during the stabilization of the megabreccia. The southernmost normal fault cut the saucer-shaped sill, indicating that megabreccia stabilization was long enough to allow its cooling and solidification. Enlarging horst formation can be understood as resulting from the inflation of the upper magma chamber, probably due to a very rapid magmatic ascent compensating the unloading produced by the explosion. The magma chamber clearly replaced the enclosing limestones, that fell and were deformed as blocks or layers in the magma.

- After the stabilization of the megabreccia, minor phreatomagmatic explosions and projections still occurred, and fed the overlying tuffs and breccia. It indicates that magma still locally met the sea water or soft sediments. However, no eruptive structures like vents or diatremes were observed across the megabreccia. These structures were probably discontinuous along the eruptive line, and the eruptions smaller by several order of magnitude than the initial one. The projections from the eruptive line consisted mainly in carbonates with a minor proportion of magmatic materials. Eruptions involved a mix of lime mud, brecciated sediments, magma and steam. Corrosion and oxidation of magmatic shards indicate a pulverization of the magma in an oxidizing environment, probably at the time of contact between magma and steam. These corroded shards, together with other projected objects as spinel crystals or sedimentary fragments were wrapped within the eruption cloud by a rim of heated mud.

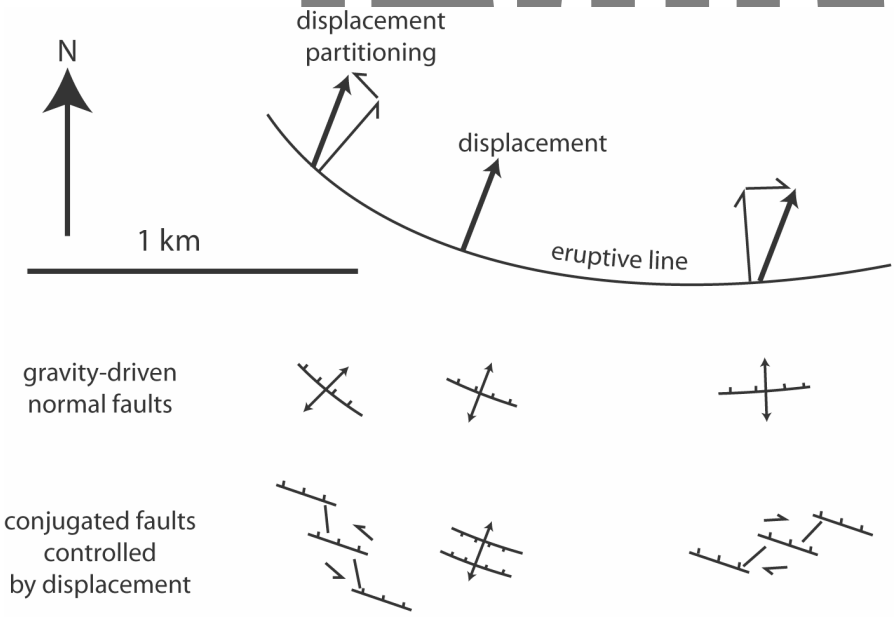

Figure 12: Map view of the inferred eruptive line. Changes in fault strike are interpreted as an effect of displacement partitioning along an arcuated eruptive line. See text for comments.

During this first phase, the carbonate platform slided above ductile magma near the eruptive line. Rapidly, the magma closest to the surface cooled and became solid, but the platform was still sliding northeastward on the underlying Matbat sediments and on the lower magma chamber that was cooling more slowly than the upper one.

- Finally, when both magmatism and displacements stopped, the calcareous sedimentation proceeded again, and sealed the whole structure. At that time the eruptive line was probably a few meters-deep trough, where platty limestones deposited. Differential compaction locally increased and maintained the subsidence along the eruptive line, and explains the gravity-driven deformations that occurred during the platty limestones deposition. The calcareous sedimentation proceeded homogeneously from the bottom of

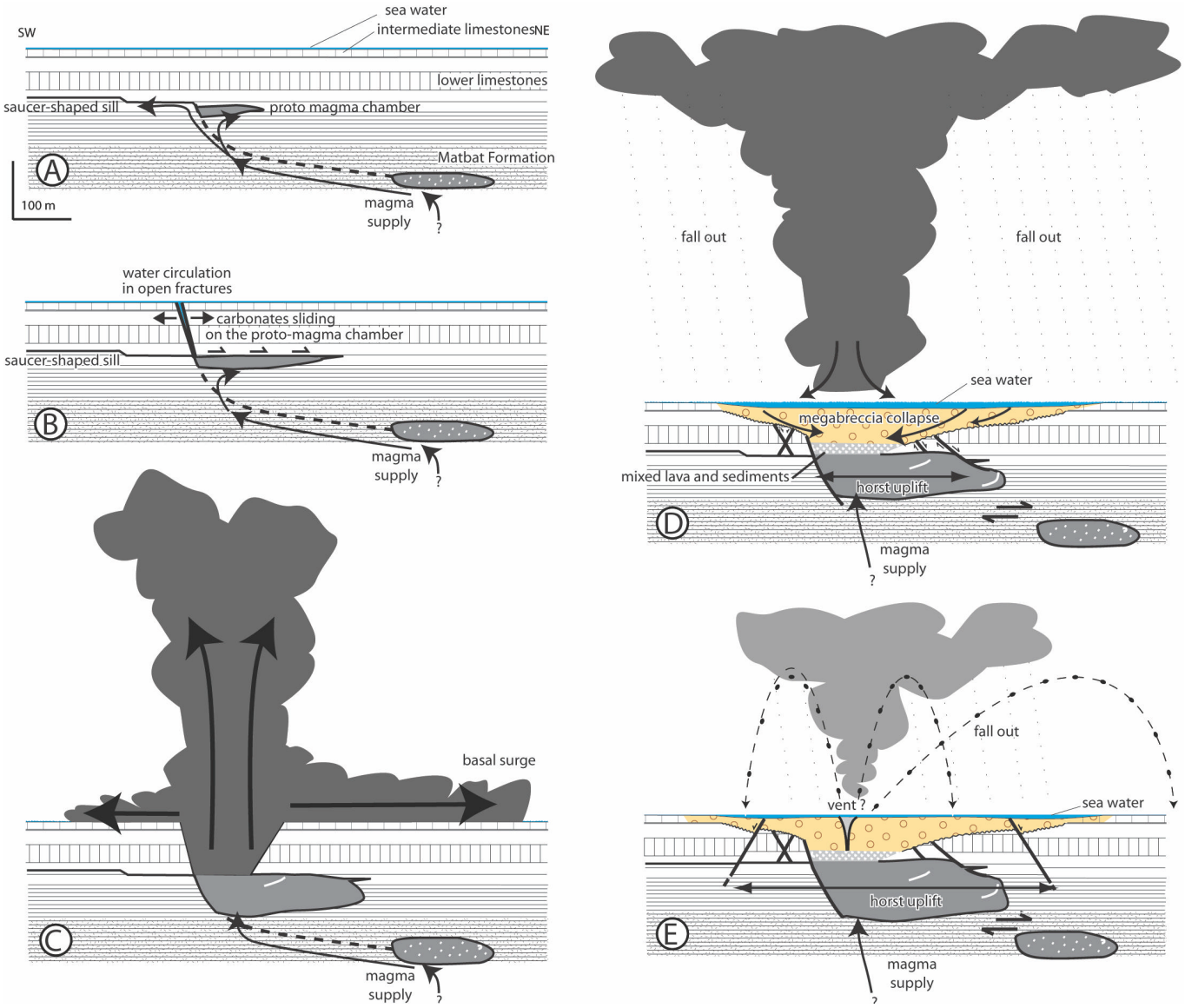

Figure 13: Reconstitution of the successive stages of eruption. Stage E corresponds to Figure 4. Dotted lines and question marks indicate inferred - but not observed - structures. See text for comments.

the upper limestones, with no significant lateral variations of facies nor thicknesses. Subsequent deformations and magmatic events obviously deformed this structure later-on, as the N-S dikes and veins cross-cutting the upper magma chamber.

DISCUSSION

Eruption style

In this paper we described only one magmatic event among the numerous eruptions or intrusions that occurred within the Triassic Misfah platform. However, the carbonate accumulation on the platform was fast enough to individualize each magmatic event, on surface and as at depth. One of the most interesting points to discuss in the studied example is the interaction between the carbonate platform and the volcanism, and how this sedimentary environment may modify the eruptive style by reference to well known types such as maars (e.g. Lorenz, 1974) or Surtsey-type eruption (Cole et al., 2001). In these two hydromagmatic types, the eruptive style is controled by magma-water interaction either above or below sea level. The vaporization of either phreatic or sea water in contact with the magma leads to violent explosions, to volcanic structures well-expressed in the topography (crater above a diatreme, tuf ring or scoria cone), and to characteristic volcanic formations or rock types (basal surge deposits, projections, hyaloclastites, palagonite).

While the eruption occurred in a marine environment, it may seem paradoxal that no structures or rock indicating a Surtsey-type eruption has been found in the studied area. There is no lava flows and a very restricted proportion of hyaloclastite or palagonite in the volcanic projections. Almost no magma reached the sea floor and cooled in contact with sea water, while a huge magmatic volume was emplaced only few tens of meters below the sea floor. The eruption seems to have been almost purely phreatic, but there is no morphologic indication of a tuf ring that may have been well-recorded in carbonate platform environment. Furthermore,

there were no repeated phreatic eruptions at depth and associated brecciated pipe, as it may be expected if the sea water could refill an aquifer in contact with the magma.

In fact, carbonate sedimentation is almost not disturbed by volcanism, but influences the eruptive style, and partly controls the intrusions. In return the magmatism controls the deformation of the host rocks. Two phenomena can explain this specific evolution:

- At surface, and after the initial phreati explosion, the megabreccia slided towards the eruptive line, creating a lid that isolated the underlying magma from the overlying sea water. The interaction of the magma with the water contained in the megabreccia (especially in the carbonate mud matrix) may have produced small and secondary phreatomagmatic eruptions and projections. These eruptions were restricted to the top of the magma chamber, which was in the eruptive line only few tens of meters below sea floor. The eruptive mechanism appears not only related to magma-water interaction, but also to the rheology of the enclosing rocks. Early diagenesis of limestones, especially dolomites, allow sedimentary layers or formations to slide like rafts during the magmatic event. Unlike soft sediments that mainly collapse and are mixed with magma during the eruptions (e.g. Sohn and Park, 2005), the displacements of these solid rafts may strongly control both geometry and evolution of the magmatic intrusion and eruption. These displacements localize the eruptive line, but the main consequence of sediment rafting is in fact to restrict the contact between magma and sea-water, and consequently the access of most of magma to the surface. In this case, magma emplacement is not controlled by explosive processes (magma-water interaction), but by gravity-driven processes (destabilization of the sedimentary cover).

- The initial phreatomagmatic explosion locally removed the topmost formations. It induced a pressure fall at depth, that allowed the ascent of a significant volume of magma and its emplacement below the lower limestones. The absence of diatreme indicates that no other explosions occurred at depth, probably because the rising magma leaved no room for breccias where water can refill an aquifer. This magma represented a decollement layer where the limestones could slide away from the eruptive line. Sliding increased the unloading along the eruptive line, allowing more magma to be emplaced at shallow depth. Rising magma produces a tectonic instability, that in return favours the magma ascent in a feedback mechanism. Comparable feedback has been proposed for the emplacement of magmatic domes as the Mt St. Helens one (Lipman and Mullineaux, 1981). In this pelean eruption, the emplacement of a crypto-dome at depth triggered a tectonic instability (gravitational sliding on the volcano flanks), that induced the blast by decompression of the unroofed crypto-dome.

The eruption induced very limited changes in the carbonate sedimentation. Of course, at the time of the eruption, carbonate sedimentation probably locally ceased, and only previously formed sediments are reworked. One may expect vertical displacements and carbonate facies changes associated to the volcanic event, but they appear to be restricted. The sub-surface intrusions are mainly compensated by the disparition of the overlying sediments, either from the eruption or by sliding. Local uplift above the eruptive line can be estimated from the slip on normal faults: it represents no more than 20% of the observed thickness of the upper magma chamber, and this displacement is almost totally absorbed within the megabreccia. The only significant effect on sedimentation is a local increase of depth and subsidence along the eruptive line allowing deposition of platy limestones. This change does not seem to be strictly related to the eruption, but mainly to the compaction of the megabreccia that filled the eruptive line.

Implications on palinspatic reconstitutions

The observations presented in this paper have also implications on the reconstitutions of the Oman continental margin during Triassic times. Until now, the nature of the basement of the Triassic exotic platform was unknown because of the decollement of the Kwar Group below the Sumail ophiolites (Fig. 1). In the studied area, the magma chambers strengthened the sedimentary section, avoiding the thrust localization at the bottom of the thick and competent Kwar Group. The presence of sediments attributed to the Matbat formation in contact with and inside the magma chambers indicates that the Kwar Group developped above pelagic sediments deposited in the Hawasina basin, i.d. the deep part of the continental margin. The basement of Oman exotics was not oceanic crust (Searle and Graham, 1982; Stampfli et al., 1991; Pillevuit, 1993; Pillevuit et al., 1997), nor the crest of a horst inherited from the permian rifting (Bechennec, 1988; Bechennec et al., 1988).

The sedimentary nature of the basement implies that there was not a thick pile of volcanic rocks beneath the Kwar Group: the the Triassic carbonate platform did not developped on an accumulation of volcanic rocks such as a volcanic island, but on an uplifted part of the continental margin. Neither the orientation of the uplifted zone nor its origin can be discussed at this point, as these questions will need to investigate the geometry of the uplifted area and its relationships with the adjacent and deeper parts of the basin, both strongly modified by the Late Cretaceous obduction.

Anyway, whatever the uplift mechanism may be, it implies a reactivation of the Oman continental margin during Middle-Late Trias. It is noteworthy that in the same Middle to Late Triassic time, magmatism occurred all along the northern edge of Gondwana (Sengör et al., 1993), from northwest Australia (Exon et al., 1982), to north India (Reuber et al., 1987), Oman, Iran (Berberian and King, 1981), and the western mediterranean area (Syria: Al-Riyami et al., 2000; Cyprus: Lapierre, 1975,

Lapierre and Rocci, 1976; Turkey: Robertson and Waldron, 1990). Rather than a Permian (Stampfli et al., 1991) or Triassic (Kazmin et al., 1986) single-stage rifting, one may propose that a major reorganization of oceanic accretion in the tethyan realm occurred at the end of Trias. Ricou (1994) proposed such a reorganization as a poorly constrained working hypothesis: during Permian times displacement of the Cimerian blocks were supposed to be mainly parallel to the Gondwana edge, and oceanic accretion occurred in a narrow ocean between transform continental margins; since Late Triassic times, continental margins were reactivated by divergence, and the oceanic realm widened. This change may also be related to the Late Triassic rifting between India and Arabia (Hauser et al., 2002).

Carbon dioxide release

Finally, one can investigate if the volcanic relelase of CO_2 in the atmosphere can be significantly modified by interactions between magma and carbonates. Large igneous provinces correlate with global climatic changes (e.g. Wignal, 2001). Volcanic gas releases in the atmosphere certainly contribute to these changes, but the involved mechanisms are not well understood. From the study of historical eruptions, short-term cooling processes controlled by SO_2 degassing (Sigurdsson, 1990) have been advantaged. However, long-term global warming and associated elevated atmospheric CO_2 concentrations have been evidenced in the biological crisis associated to the Siberian traps (Permian-Trias boundary), Central Atlantic Magmatic Province (Trias-Jurassic boundary) and Karoo traps (Early Toarcian) (Wignal, 2001).

Until now, estimates of CO_2 degassing from lavas were based either on direct measurements (Hawaï: $5\ 10^{12}$ g of CO_2 for 1 km^3 of lava, McCartney et al., 1990) or from CO_2 contents in lavas (e.g. McHone, 2003: $2.2\ 10^{12}$ g of CO_2 for 1 km^3 of lava), to be compared with $3.5\ 10^{12}$ g of CO_2 for 1 km^3 of lava from Leavitt's (1982) empirical formula. Carbon dioxide emissions was estimated to 2.6 to 8.8 and $5.2\ 10^{18}$ g for the Deccan trapps (Caldeira and Rampino, 1990) and the Central Atlantic Magmatic Province (McHone, 2003), respectively. These huge amounts are almost at the same magnitude of the $5\ 10^{19}$ g of CO_2 stocked in the atmosphere and oceans; but once reported to the duration of the magmatic events, they appear quite small when compared to the current anthropogenic CO_2 release (10^{16} g $year^{-1}$, Leavitt, 1982). Limestones represent the main reservoir in the atmospheric cycle of Carbon: one cubic kilometer of $CaCO_3$ (density 2.5) represents $1.1\ 10^{15}$ g of CO_2. If a basaltic intrusion replaces carbonated sediments, CO_2 release can be two to three hundred times greater than simply degassing of lavas reaching the surface.

In the studied example, there is many evidences that the upper magma chamber replaces the enclosing limestones. Deformations can explain only a restricted part of the volume of the magma chamber: horst uplift has been estimated to 20% of lava thickness (see above), horizontal stretching was probably also limited, as the normal faults exhibit only small offsets, and the shear zone between the two magma chambers shows only limited strain. As for the vertical displacements, a conservative estimate may be that only 20% of the magma chamber width can be explained by stretching. The upper magma chamber is 300 meters-wide, 100 meters-high (Fig. 4), and probably at least one kilometer long (Figs. 3 and 12). Assuming that 20% of height and width have been created by sediment deformation, magma replaced a volume of 0.019 km^3 of limestones, that represents a rough estimate of $3.5\ 10^{13}$ g of CO_2. It underestimates the intrusion size, which is based mainly on the present day outcrops, but overestimates the CO_2 release, considering the replaced rocks as only $CaCO_3$, and not taking in account the volume of limestones xenoliths remaining in the magma, nor the Carbon that may have been incorporated in the magma. The exact mechanisms of CO_2 release from the carbonates interacting with the magmatic intrusion are still to be studied.

However, this source of CO_2 release from magmatic intrusions may have been of prime importance in global climatic changes. It was not the case of the studied event, which was negligible at global scale. However the question must be investigated at least in the case of the three magmatic events clearly associated to important increase in atmospheric CO_2 (Wignal, 2001): the Permian-Triassic Siberian traps, the Triassic-Jurassic Central Atlantic Magmatic Province, and the Early Toarcian Karoo-Ferar magmatism. In these three cases, the intruded magmatic volumes were huge, for example 550 000 km^3 in the Central Atlantic Magmatic Province (McHone, 2003), including 360 000 km^3 in the Amazonian basin alone (Almeida, 1986). If only a small part of these intrusions replaced carbonated sediments, and consequently released Carbon dioxide, it may considerably change the present-day estimates of CO_2 releases in these large igneous provinces: decarbonating of limestones in only 1% of the volume of intrusions in the Central Atlantic Magmatic Province represent 10^{19} g of CO_2, to be compared to the $5.2\ 10^{18}$ g of CO_2 estimated from magma degassing for the whole Province. As in the case of the Paleogene climatic change, where magmatic intrusions in the Vöring Basin have been proposed as driving mechanism (Svensen et al., 2004), the key explanation of global climatic changes associated to the largest magmatic events may be hidden below the surface rather than in effusives flows.

Acknowlegdements

This paper is dedicated to our colleague Henriette Lapierre, deceased in January 2006, and who initiated our work in Oman. The field work has been partially funded by the Groupement de Recherche 'Marges'. The Centre National de Recherche Scientifique and Université Joseph Fourier also provided financial support, together with various funds initially scheduled for other scientific works. Writing by C.B. has been partly done during a leave for health

reasons. We thank F. Béchennec and N. Arndt for very fruitfull discussions at various stages of this work, and Dr Hilal Mohammed Sultan Al Azri from omani Ministry of Commerce and Industry for his kind welcome and support in Oman. Rose diagrams and stereo nets were drawn using A. Pecher's Stem software. By reference to the goat that joined us in the magma chamber, we shall appreciate if this volcanic event and the associated structures will be named Goat's Volcano.

References

Almeida, F.F.M. de, 1986, Distribuição regional e relações tectônicas do magmatismo pós-Paleozóico no Brasil: Revista Brasileira de Geociencias, v. 16, p. 325-349.

Al-Riyami, K., Robertson, A.H.F., Xenophontos, C., Danielan, T., Dixon, J.E., 2000, Tectonic evolution of the Mesozoic Arabian passive continental margin and related ophiolite in Baer-Bassit region (NW Syria), *in* Panayides, I. et al., eds: Proceedings of the Third International Conference on the Geology of the Eastern Mediterranean, p. 61-81.

Baud, A., Béchennec, F., Cordey, F., Krystyn, L., Le Métour, J., Marcoux, J., Maury, R., Richoz, S., 2001, Permo-Triassic deposits: from the platform to the basin and seamounts: International Conference on the Geology of Oman, Excursion n°A01, 56 p.

Béchennec, F., 1988, Géologie des nappes Hawasina dans les parties orientales et centrales des montagnes d'Oman: Documents BRGM, v. 127, 474 p.

Béchennec, F., Le Métour, J., Rabu, D., Villey, M., and Beurrier, M., 1988, The Hawasina Basin: a fragment of a starved passive continental margin, thrust over the Arabian Platform during obduction of the Sumail Nappe: Tectonophysics, v. 151, p. 323-343.

Béchennec, F., Le Métour, J., Rabu, D., Bourdillon-Jeudy de Grissac, C., De Wever, P., Beurrier, M., and Villey, M., 1990, The Hawasina Nappes: stratigraphy, paleogeography, and structural evolution of a fragment of the south-Tethyan passive continental margin, *in* Robertson, A.H.F. et al. (eds), The geology and tectonics of the Oman region: Geological Society Special Publications, v. 49, p. 213-224.

Béchennec, F., Tegyey, M., Le Métour, J., Lemière, B., Lescuyer, J.L., Rabu, D., and Milesi, J.P., 1991, Igneous rocks in the Hawasina Nappes and the Al-Hajar supergroup, Oman mountains: their significance in the birth and evolution of the composite extensional margin of eastern Tethys, *in* Peters, T. et al., eds, Ophiolite genesis and evolution of the oceanic lithosphere: Kluwer Academy, Norwell, Massachuset, p. 569-611.

Beltramo, J., 2003, Les séries carbonatées crétacées d'arc volcanique du Terrane Guerrero (Mexique): Ph-D Thesis, Université Joseph Fourier, Grenoble, France, 296 p.

Berberian, M., and King, G.C.P., 1981, Towards a paleogeography and tectonic evolution of Iran: Canadian Journal of Earth Sciences, v. 18, p. 210-265.

Beurrier, M., Béchennec, F., Rabu, D., and Hutin, G., 1986, Geological map of Rustaq: Sheet NF40-3A, Scale 1/100 000, Sultanate of Oman, Ministry of Petroleum and Minerals, Directorate General of Minerals, BRGM, Orléans, Editeur.

Buigues, D., Gachon, A., and Guille, G., 1992, L'atoll de Mururoa (Polynésie française) I. – Structure et évolution géologique: Bulletin de la Société Géologique de France, v. 163, p. 645-657.

Caldeira, K., and Rampino, M.R., 1990, Carbon-dioxide emissions from Deccan volcanism and a K/T boundary greenhouse-effect: Geophysical Research Letters, v. 17, p. 1299-1302.

Chevallier, L., and Woodford, A., 1999, Morpho-tectonics and mechanism of emplacement of the dolerite rings and sills of the western Karoo, South Africa: South African Journal of Geology, v. 102, p. 43-54.

Cole, P.D., Guest, J.E., Duncan, A.M., and Pacheco, J.M., 2001, Capelinhos 1957-1958, Faial, Azores: deposits formed by an emergent surtseyan eruption: Bulletin of Volcanology, v. 63, p. 204-220.

Exon, N.F., von Rad, U., and von Stackelberg, U., 1982, The geological development of the passive margin of the Exmouth Plateau off Northwest Australia: Marine Geology, v. 47, p. 131-152.

Fisher, R.V., 1977, Erosion by volcanic base-surge density currents: U-shaped channels: Geological Society of America Bulletin, v. 88, p. 1287-1297.

Fulthorpe, C.S., and Schlanger, S.O., 1989, Paleo-oceanographic and tectonic settings of Early Miocene reefs and associated carbonates of offshore southeast Asia: American Association of Petroleum Geologist Bulletin, v. 73, p. 729-756.

Glennie, K.W., Bœuf, M.G.A., Hughes Clarke, M.W., Moody-Stuart, M., Pillaart, W.F.H., and Reinhart, B.M., 1973, Late Cretaceous nappes in the Oman mountains and their geologic significance: American Association of Petroleum Geologist Bulletin, v. 57, p. 5-27.

Glennie, K.W., Bœuf, M.G.A., Hughes Clarke, M.W., Moody-Stuart, M., Pillaart, W.F.H., and Reinhart, B.M., 1974, Geology of the Oman mountains: Geologisch Mijnbouwkundig, v. 1, 423 p.

Graham,G.M., 1980, Structure and sedimentation of the Hawasina window, Oman mountains, Ph. D. Thesis: Milton Keynes, England, Open University, 422 p.

Hamilton, E.L., 1956, Sunken islands of the Mid-Pacific Mountains: Memoir of the Geological Society of America, v. 64.

Hauser, M., Martini, R., Matter, A., Krystyn, L., Peters, T., Stampfli, G., and Zaninetti, L., 2002, The break-up of East Gondwana along the northeast coast of Oman: evidence from the Batain basin: Geological Magazine, v. 139, p. 145-157.

Hess, H.H., 1946, Drowned ancient islands of the Pacific basin: American Journal of Sciences, v. 244, p. 772-791.

Kazmin, V., Ricou, L.E., and Sbortshikov, I.M., 1986, Structure and evolution of the passive margin of the eastern Tethys: Tectonophysics, v. 123, p. 153-179.

Lapierre, H., 1975, Les formations sédimentaires et éruptives des nappes de Mamonia et leurs relations avec le Massif du Troodos (Chypre occidentale): Mémoire de la Société Géologique de France, v. 123, 127 p.

Lapierre, H., and Rocci, G.M., 1976, Le volcanisme alcalin du Sud-Ouest de Chypre et le problème de l'ouverture des régions téthysiennes au Trias: Tectonophysics, 30, p. 299-313.

Larue, D.K., Smith, A.L., and Schellekens, J.H., 1991, Oceanic island arc stratigraphy in the Carribean region: Sedimentary Geology, v. 74, p. 289-308.

Leavitt, S.W., 1982, Annual volcanic carbon dioxide emission: an estimate from eruption chronologies: Environmental Geology, v. 4, p. 15-21.

Lipman P.W., and Mullineaux, D.R. (eds.), 1981, the 1980 eruptions of Mount St. Helens, US Geological Survey Professional Paper 1250, 844 p.

Lorenz, V., 1974, On the formation of maars: Bulletin of Volcanology, v. 37, p. 183-204.

Martin, U., Breitkreuz, C., Egenhoff, S., Enos, P., and Jansa, L., 2004, Shallow-marine phreatomagmatic eruptions through a semi-solidified carbonate platform (ODP Leg 144, Site 878, Early Cretaceous, MIT Guyot, West Pacific): Marine Geology, v. 204, p. 251-272.

Matthews, J.L., Heezen, B.C., Catalano, R., Coogan, A., Tharp, M., Natland, J., and Rawson, M., 1974, Cretaceous drowning of reefs on Mid-Pacific and Japanese guyots: Science, v. 184, p. 462-464.

McCartney, K., Huffman, A.R., and Tredoux, M., 1990, A paradigm for endogenous causation of mass extinctions, *in* Sharpton, V.L. et al., eds, Global catastrophes in earth history: Geological Society of America, Special Paper, v. 247, p. 125-138.

McHone, J.G., 2003, Volatile emissions from Central Atlantic Magmatic Province basalts: mass assumptions and environmental consequences, *in* Hames, W. et al., eds, The Central Atlantic Magmatic Province: insights from fragments of Pangea: Geophysical Monograph, v. 136, p. 241-254.

Pillevuit, A., 1993, Les blocs exotiques du sultanat d'Oman, évolution paléogéographique d'une marge passive flexurale: Ph-D thesis, Mémoires de Géologie, Lausanne, v. 17, 249 p.

Pillevuit, A., Marcoux, J., Stampfli, G., and Baud, A., 1997, The Oman exotics: a key to the understanding of the Neotethyan geodynamic evolution: Geodinamica Acta, v. 10, p. 209-238.

Premoli Silva, I., Haggerty, J., Rack, F., et al., 1993, Proceedings ODP, Initial Reports, v. 144: College Station, TX (Ocean Drilling Program), 1084 p.

Reuber, I., Colchen, M., and Mevel, C., 1987, The geodynamic evolution of the South-Tethyan margin in Zanskar, NW-Himalay, as revealed by the Spontang ophiolitic melanges: Geodinamica Acta, v. 1, p. 283-296.

Ricou, L.E., 1994, Tethys reconstructed: plates, continental fragments and their boundaries since 260 Ma from Central America to South-eastern Asia: Geodinamica Acta, v. 7, p. 169-218.

Robertson, A.H.F., and Searle, M.P., 1990, The northern Oman Tethyan continental margin: stratigraphy, structure, concepts, and controversis, *in* Robertson, A.H.F. et al. (eds), The geology and tectonics of the Oman region: Geological Society Special Publications, v. 49, p. 3-25.

Robertson, A.H.F, and Waldron, J.W.F., 1990, Geochemistry and tectonic setting of Late Triassic and Late Jurassic-Early Cretaceous basaltic extrusives from the Antalya Complex, south west Turkey, *in*: Savascin, M.Y., et al., eds, International Earth Sciences Congress on Aegean Region, Proceedings 2, p. 279-299.

Sager, W.W., Winterer, E.L., Firth, J.V., et al., 1993, Proceedings ODP, Inititial Reports, v. 143: College Station, TX (Ocean Drilling Program), 724 p.

Schlager, W., 1981, The paradox of drowned reefs and carbonate platforms: Geological Society of America Bulletin, v. 92, p. 197-211.

Searle, M.P., and Graham, G.M., 1982, "Oman exotics" – Oceanic carbonate build-ups associated with the early stage of continental rifting: Geology, v. 10, p. 43-49.

Sengör, A.M.C., Cin, A., Rowley, D.B., and Nie, S.Y., 1993, Space-time patterns of magmatism along the Tethysides: a preliminary study: The Journal of Geology, v. 101, p. 51-84.

Shipboard Scientific Party, 1993, Site 878, *in* Premoli Silva, I., Haggerty, J., Rack, F., et al., Proceedings ODP, Initial Reports, v. 144: College Station, TX (Ocean Drilling Program), p. 331-412.

Sigurdsson, H., 1990, Evidence for volcanic loading of the atmosphere and climatic response: Palaeogeography, Palaeoclimatology, Palaeoecology, v. 89, p. 277-289.

Sohn, Y.K., and Park, K.H., 2005, composite tuff ring/cone complexes in Jeju Island, Korea: possible consequences of substrate collapse and vent migration: Journal of Volcanology and Geothermal Research, v. 141, p. 157-175.

Soja, C.M., 1996, Island-arc carbonates; characterization and recognition in the ancient geologic record: Earth Science Reviews, v. 41, p. 31-65.

Stampfli, G., Marcoux, J., and Baud, A., 1991, Tethyan margins in space and time: Palaeogeography, Palaeoclimatology, Palaeoecology, v. 87, p. 373-409.

Svensen, H., Planke, S., Malthe-Sorenssen, A., Jamtveit, B., Myklebust, R., Eidem, T.R., and Rey, S.S., 2004, Release of methane from a volcanic basin as a mechanism for initial Eocene global warming: Nature, v. 429, p. 542-545.

Thomson, K., and Hutton, D., 2004, Geometry and growth of sill complexes: insights using 3D seismic from the North Rockall Trough: Bulletin of Volcanology, v. 66, p. 364-375.

Watkins, R., 1993, Permian carbonate platform development in an island-arc setting, Eastern Klamath terrane, California: The Journal of Geology, v. 101, p. 659-666.

Wignall, P.B., 2001, Large igneous provinces and mass extinctions: Earth Science Reviews, v. 53, p. 1-33.